Check for updates

Cleaning performance of stainless steel surfaces fouled with preheated starch-protein binary mixtures: Mechanical properties, removal mechanisms, and in-place cleaning

Alejandro Avila-Sierra [a,b,*], Raquel Montoya-Guzman [a,c], Zhenyu J. Zhang [a], Peter J. Fryer [a], Jose M. Vicaria [c]

[a] School of Chemical Engineering, University of Birmingham, B15 2TT Birmingham, United Kingdom
[b] Université Paris-Saclay, INRAe, AgroParisTech, UMR SayFood, 91120 Palaiseau, France
[c] Chemical Engineering Department, University of Granada, Avda. Fuentenueva, s/n, 18071 Granada, Spain

ABSTRACT

In the food industry, deposits are often composed of multiple components and micro-structures for which removal may diverge from conventional cleaning protocols. Incomplete removal of those deposits may compromise hygiene of manufacturing lines and impact product quality. Here, we investigated the cleaning performance of model foulants made from mixtures of starch and protein adhered to stainless steel surfaces, assessing their viscoelastic properties, removal mechanisms, and cleaning effectiveness in response to different standard chemical treatments (pH 7 and pH 13) and cleaning temperatures (20 and 40 °C). Deposits displayed distinct viscoelastic behaviours under mechanical stress, affecting their removal mechanisms, especially during in-place cleaning. Young's modulus data correlated with the cleaning efficiency of the model foulants. Notably, a decrease in deposit hardness was associated with easier detachment from the metal surface for starch-rich deposits (P0 and P30, 100% and 70% starch gel respectively). In contrast, protein-rich deposits, particularly P80 (80% protein gel-20% starch gel), required greater removal forces. This was especially evident in the absence of chemical treatment, where P80 demanded more effort to be removed compared to all other deposits. The use of chemical treatment reduced the mechanical stress and removal work needed for cleaning, alkaline treatment being effective for most deposits. Alkaline cleaning was efficient at removing protein and starch-based foulants, especially for the sole protein or sole starch-containing deposits. However, P80 exhibited similar removal levels at both pH 7 and pH 13. Therefore, this research underscores the intricate removal mechanisms for starch-protein mixtures compared to single deposits, highlighting how variations in deposit composition over time during industrial processing can impact the efficiency of current Clean-in-Place (CIP) protocols.

1. Introduction

The act of cleaning – here referring to removal of unwanted material from a surface - occurs on a daily basis on a variety of scales, in households and large industrial facilities alike. In sectors such as food, beverages, and pharmaceuticals, industrial manufacturing lines often employ Clean-In-Place (CIP) systems to uphold consistent and reproducible cleanliness standards. These standards are vital for ensuring the production of high-quality goods and maintaining hygienic conditions within the manufacturing facility. However, routine cleaning operations consume substantial resources, including materials, energy, chemicals,

and water, contributing to the environmental footprint and costs of manufacturing (Eide et al., 2003; van Asselt et al., 2005; Schug, 2016; Heldman, 2021; Huellemeier et al., 2022). The optimisation of these processes is imperative for achieving more efficient and sustainable manufacturing practices.

Cleaning effectiveness relies on a wide array of variables, encompassing factors such as the type of the foulant and surface, temperature, hydrodynamic forces, cleaning solution composition, and the duration of the cleaning process (Tanaka and Hoshino, 1999; Liu et al., 2002, 2006; von Rybinski, 2007; Boxler et al., 2013). Numerous investigations have aimed to elucidate the behaviour of model foulants during in-place

cleaning and to determine the optimal balance of temperature, chemical concentration, and mechanical force required for effective deposit removal (Gottschalk et al., 2022). Efficient cleaning necessitates the overcoming of cohesive bonds within contaminant layers and the adhesive forces between contaminants and the substrate, all while expending minimal energy, combining the action of chemicals with mechanical forces (Landel and Wilson, 2021).

Cleaning operations have been categorised based on three main factors: the hydrodynamic forces exerted by the circulating fluid, temperature, and the aggressiveness of the cleaning agents (Fryer and Asteriadou, 2009). There are three distinct deposit types: Type 1 (associated with viscous or viscoelastic fluids), Type 2 (comprising biofilms), and Type 3 (consisting of complex solids that require the use of cleaning chemicals) (Fryer et al., 2011). In the food industry, cleaning become progressively intricate due to the composition of food deposits, which are typically multi-component and micro-structured (Cuckston et al., 2019), where food compounds such as proteins (Christian and Fryer, 2006; Avila-Sierra et al., 2021a), starches (Jurado-Alameda et al., 2015), fats and other hydrophobic components (Ali et al., 2015) often lead to significant cleaning challenges during food processing. For instance, when heated, proteins and starches adhere to the inner surfaces of pipes and equipment in the plant, leading to the formation of Type 3 deposits that necessitate the application of chemical agents (alkaline solutions) and high temperatures for removal (Nor Nadiha et al., 2010; Vicaria et al., 2017; Avila-Sierra et al., 2021b). Dissolution and cleaning rates of high-protein deposits exhibit a pseudo-linear increase with alkali concentration, peaking around ~0.1 M alkali (Jennings, 1965). However, beyond this threshold, the cleaning efficacy markedly declines (Bird and Fryer, 1991; Fan et al., 2019a, 2019b; Mercadé-Prieto et al., 2008; Tuladhar et al., 2002). Contrastingly, when dealing with starches, higher alkaline concentrations typically prove more effective (Vicaria et al., 2017). This phenomenon occurs as hydroxyl ions diffuse towards the starch structure, facilitating swelling and subsequent degradation of its internal framework (Lai et al., 2004; Han and Lim, 2004).

Despite the unquestionable usefulness of Cleaning Maps (Fryer and Asteriadou, 2009), the practice of categorising deposits with varying cleaning behaviours into common groups can lead to a loss of crucial information when developing cleaning procedures, especially when dealing with real-world deposits composed of multiple compounds (Gottschalk et al., 2022). Typically, empirical cleaning correlations are established for each type of fouling material (Wilson et al., 2022). However, these correlations become challenging to apply when there are alterations in deposit composition, the inclusion of other food components, or variations in environmental conditions. Consequently, this significantly undermines the efficiency of CIP operations and the overall hygiene within the facility. Therefore, it is essential to identify and comprehend the fundamental mechanisms involved in cleaning complex and more realistic food deposits to make informed choices and enhance cleaning protocols.

When it comes to foulant mixtures, there has been limited research thus far. For example, Magens et al. (2017), using commercial baking foods, found that the removal of cake deposits from solid surfaces was highly dependent on the oil content. Herrera-Marquez et al. (2020) showed that systematic changes in the composition of starch-fat mixtures (Type 3 and Type 1, respectively) altered cleaning parameters concerning single deposits. They reported that the resistance of these complex deposits to mechanical removal shifted from strong adhesive and cohesive interactions to reduced removal forces as the starch concentration decreased, making high-fat content (≥60%) deposits easily removable at neutral pH and higher temperatures (50 °C). Recently, Saenz-Espinar et al. (2024) analysed the cleaning process of food complex deposits formed by systematic mixtures of corn starch, whey protein and lard. They found that starch gels (20% wt,/wt) required less shear stress for removal than whey-based deposits at pH 7 and under alkaline conditions. For binary mixtures, starch–whey deposits where

harder to remove with hot water. Alkaline treatment improved removal efficiency for starch-containing mixtures but decreased it for whey–lard mixtures compared to hot water treatment. The removal rate of the three-component mixture (equal fractions of each compound) generally remained ~50%, regardless the cleaning treatment employed. Notably, binary mixtures of starch-lard showed a significant change in shear stress data above a 50% lard fraction, consistent with Herrera-Marquez et al. (2020). Detergency levels varied between 30% and 80% lard fractions, depending cleaning highly on the solid concentration of the initial deposits. The mixture of starch and protein also showed varied cleaning responses based on their fractions, though this behaviour was less clear at higher solid concentrations (30% wt./wt.). In related research on wastewater treatment, Ang et al. (2011) found higher cleaning efficiency on membranes fouled with solutions containing more alginate. This was likely due to the microstructure of the deposit (i. e., higher porosity), which may enhance the transfer of cleaning agents and reaction products.

To better understand whether the cleaning response of complex food mixtures is related to their mechanical properties, a set of experiments was conducted, including micro-indentation, micro-manipulation, and in-place cleaning to provide a thorough understanding of the cleaning behaviour of different model foulants derived from starch-protein mixtures of gels (40% wt./wt.), representing Type 3 deposits. These experiments involved subjecting the foulants to thermal treatment to explore how the cleaning response varies when there are systematic changes in deposit composition compared to cleaning their individual components. The primary objectives encompassed: (i) ascertaining the viscoelastic properties of the foulants, specifically their Young's modulus, (ii) quantifying the adhesive and cohesive forces existing between the foulant and the surface or within the layers of the foulant, and (iii) gaining insights into the potential mechanisms employed for removing these model deposits.

2. Materials & methods

2.1. Materials

Five model foulants were prepared by combining soluble potato starch (CAS-No.: 9005-84-9, Panreac, Barcelona, Spain) and whey protein concentrate (WPC, Abbott, Granada, Spain), having the latter a protein content of 79.6%, carbohydrate content of 9.3%, fat content of 4.9%, ash content of 3.0%, and humidity content of 3.2%. Two aqueous cleaning solutions were employed in the study: pH 7 buffer consisting of 0.1 M monopotassium phosphate (KH_2PO_4) and 0.1 M sodium hydroxide (NaOH) with a proportion of 63.21 and 36.79% respectively, and a pH 13 alkaline solution (5.8 g/L NaOH), prepared using NaOH pellets (CAS-No: 1310-73-2, Panreac, Barcelona, Spain), representative of those used for Clean-In-Place (CIP) processes.

2.2. Model surfaces

In this work, representative surfaces from food contact settings have been selected. For the in-place cleaning experiments, new and freshly unpacked and prepared spherical coupons made of stainless steel 410 fibres (0.51 mm width) were used as the fouling substrate to mitigate the risk of potential contaminants. These coupons pose a ~2.0 cm diameter and 0.80–0.85 g weigh. Additionally, they have a remarkable 93% free volume fraction (Jurado et al., 2015). Each cleaning assay involved the use of eight of these spheres. For the micro-manipulation measurements, flat and square coupons made of stainless steel 316L, with dimensions of 2.54×2.54 cm, were chosen. These coupons exhibit an averaged surface roughness of 0.44 ± 0.08 μm (S_a; surface arithmetical mean height), well within the specified standard limits for food contact applications (Avila-Sierra et al., 2021b). To determine the surface roughness, White Light Interferometry (WLI) was employed using the MicroXAM2 instrument by KLA Tencor in California, U.S.A., gathering data from at

least three different locations on each sample. To ensure cleanliness, the micromanipulation coupons underwent a thorough cleaning process: first, they were exposed to a 2.0% (wt./wt.) NaOH aqueous solution at 80 °C with stirring for 1 h to eliminate any potential contaminants. Subsequently, they were cooled to room temperature (20 °C) using a water bath. Following this, the substrates were rinsed with a 1.0% (vol/vol) HCl solution and acetone, after which they were dried using an air stream (Avila-Sierra et al., 2021b). All solvents were HPLC grade. Differences between the stainless steel substrates used may condition adhesion forces.

2.3. Model foulants and fouling method

In this study, a series of five distinct foulant compositions, each consisting of whey protein concentrate (WPC) and potato starch (PS) at a solid concentration of 40% (wt./wt.), were prepared as indicated in Table 1. The initial protein content for each foulant, denoted as P0, P30, P60, P80, and P100, was precisely controlled to be 0%, 23.9%, 47.8%, 63.7%, and 79.6% of WPC respectively, based on a dry weight basis. The moisture content of both products was deemed negligible for the calculations. The preparation process involved combining the components in a Milli-Q water medium, followed by stirring and heating at 67 °C for 1 h to initiate the starch gelatinisation process and avoid protein denaturation in the WPC powder. Subsequently, the solutions were gradually cooled to 20 °C over a 24-h period to facilitate retrogradation, ensuring the attainment of the desired foulant characteristics.

Anticipating potential variations in adhesion compared to industrial deposits, we chose to initially subject the model foulants to thermal treatment. Subsequently, we allowed them to adhere to the specified surfaces, creating reproducible foulants. To conduct the fouling experiments, spherical coupons (section 2.2) were deliberately exposed to and rolled within the specific model foulant of interest. Each sphere was weighted, retaining a consistent amount of 2.0 ± 0.5 g of the foulant material. For the flat and square coupons (section 2.2), a standard holder measuring 2.5 × 2.5 × 1 cm was employed to maintain a uniform and fixed quantity of the foulant during the fouling process. The resulting samples achieved a final height of approximately 10 mm, ensuring standardisation for subsequent analyses. Before conducting the cleaning tests, the fouled substrates were incubated in a sealed container (silica gel-free) at 4 °C for 30 min. Representative images of the fouled surfaces are depicted in Fig. 1.

2.4. Micro-indentation analysis

For the determination of the viscoelastic properties of the model foulants, a bespoke micro-indentation system, a derivation of the micro-manipulation device detailed in section 2.5, was developed at the University of Birmingham. This apparatus employed a conical probe with an angle of 40°, moving on the normal direction, while a force transducer records the load as a function of depth. The resulting load *vs.* displacement curves provide information of the mechanical nature of the samples under study. The effective approach rate was set at 1 mm/s, commencing from a vertical distance of 11 mm. A predetermined set-point force of 5 N (±0.001 N) was established, attained at the precise

Table 1

Composition of the model foulants, comprising a combination of potato starch (PS) and whey protein (WPC), wherein "P" alludes to the relative concentration of the protein component.

Foulant	WPC/%	PS/%
P0	0	100
P30	30	70
P60	60	40
P80	80	20
P100	100	0

moment when the conical probe gently made contact with the metal surface. These measurements were conducted under two distinct temperature conditions: one at room temperature (20 °C) and the other at a moderate cleaning operation temperature (40 °C). Samples were first brought to room temperature and then conditioned to the testing temperature for 5 min before each experimental run. The final reported results were the outcome of averaging, with a minimum of three repetitions. Various batches of the model foulants have been prepared and used to conduct the respective measurements.

For the computation of the Young's modulus, the maximum indentation depth did not surpass 40% of the deposit thickness, thereby effectively mitigating any potential influence stemming from the underlying metal substrate. The well-known Sneddon indentation model (Sneddon, 1948), applied for the conical indenter, was used for analysis:

$$F = \frac{2}{\pi} \frac{E}{(1-\nu^2)} \tan(\alpha) \delta^2 \qquad \text{Eq. (1)}$$

where F represents the recorded force, while E is the Young's modulus, considered a fitting parameter. The Poisson's ratio, ν, held estimated to be constant at 0.47 for the model deposits, aligning with those reported for starch and whey protein gels in previous works (Langley and Green, 1989; Palanisamy et al., 2022). Additionally, the indenter's half-angle (α) and the indentation depth (δ) are also considered in this model, assuming a contact area of ~1.4 cm^2.

2.5. Micro-manipulation measurement

Micro-manipulation, as first expounded by Liu et al. (2002), was employed to investigate the intricate mechanisms governing the mechanical removal of model foulants firmly adhered to stainless steel surfaces. The method involved employing a finely calibrated device that possessed the capability to gauge the force required (sensitivity of 0.001N) to remove the deposit from the surface, revealing the adhesion forces, or to eliminate a layer thereof, thereby unveiling the cohesion forces. This sample holder travels at a velocity of 1 mm/s, while a precision blade scraped the deposit at approximately 5 mm and 1 mm from the surface for "cohesive" and "adhesive" measurement levels, respectively. It is important to recognise that in this study, the forces identified at the cohesive level or adhesive level may not conclusively represent the removal mechanisms of deposits during mechanical cleaning, as they may involve a combination of factors. The force (mN), mandated to effectively remove the deposit, was recorded as a function of time. The micro-mechanical removal of the five model foulants tested in this work was conducted in an ambient environment (air), as a control case, and under different cleaning conditions (pH 7 and pH 13), at two different temperatures (20 and 40 °C). In air, samples were first brought to room temperature and then conditioned to the testing temperature for 5 min before each experimental run. The temperature of the cleaning solution was controlled through the temperature-regulated sample holder stage which featured a glass window to allow for *in-situ* observation. This multifaceted stage was designed with five interconnected compartments. Prior to testing, all samples were immersed in the cleaning solution at the temperature of interest for a duration of 20 min, preparing them for the subsequent assessments. The experiments were replicated at least three times. Various batches of the model foulants have been prepared and used to conduct the respective measurements.

From each force profile, two essential removal parameters were computed: (i) the deposit peak force ($F_{\max}$) which was converted to the maximum shear stress ($\tau_{\max}$) dividing by the contact area of the deposit-surface interface (A), and (ii) the breakage work per area (W_b) defined as:

$$Wb = \frac{1}{A} \int_{to}^{t1} F(t) \bullet dx \qquad \text{Eq. (2)}$$

Where $F(t)$ was the measured force, and t_o and t_1 are the start and end

Fig. 1. The visual representation captures the assortment of model foulants subjected to experimentation, arranged from left to right as follows: P0 (100% starch gel), P30, P60, P80, and P100 (100% whey protein gel). These samples are placed on a flat metal surface with dimensions measuring 2.5 × 2.5 cm.

times of the experiment (Herrera-Marquez et al., 2020).

2.6. Lab-simulated in-place cleaning

Cleaning evaluations were executed using a laboratory-simulated Clean-In-Place (CIP) system (Fig. 2) (Vicaria et al., 2017), which featured a tank with a volumetric capacity of 1 L, a peristaltic pump supplying a flow rate of 120 L/h, and a glass column (diameter: 2.5 cm, height: 8.5 cm, capacity: 50 mL). For each cleaning test, 1.2 L of the cleaning solution was introduced into the tank and recirculated until the desired temperature was attained. Subsequently, with temperature equilibrium achieved, the peristaltic pump ceased its operation, allowing the placement of eight fouled spheres into the glass column. The initial mass of deposit on the spheres was measured, exhibiting a total of foulant of 16.0 ± 1.0 g for each cleaning test. Initiating the cleaning assay, the peristaltic pump was reactivated, recirculating the washing solution through the CIP system for 15 min. Upon the completion of the cleaning process, the peristaltic pump was halted, followed by the extraction of the treated spheres from the device, spheres were then dried for 24 h at 60 °C, and weighed together.

The total detergency of the mixed deposit (De, %) was evaluated according to Eq. (3):

$$De\ (\%) = \frac{m_0 - m_f}{m_0}\ x\ 100 \qquad \text{Eq. (3)}$$

where m_o and m_f are the deposit mass (in dry weight) before and after cleaning, respectively, so that 100% is complete removal. Tests are made by triplicate.

The protein cleaning rate (PCR) (i.e., percentage of protein that is removed during cleaning) is evaluated as:

$$PCR\ (\%) = \frac{m_{o\ protein} - m_{f\ protein}}{m_{o\ protein}}\ x\ 100 \qquad \text{Eq. (4)}$$

where $m_{o\ protein}$ and $m_{f\ protein}$ are the difference between the protein mass before and after cleaning, respectively.

The quantification of protein concentration was accomplished using the BCA Protein Assay Kit (ThermoFisher Scientific, Madrid, Spain), which encompasses the components BCA Reagent A and BCA Reagent B. In this analytical process, samples of 25 μL, formulated in a pH 7 solution were positioned within a spectrophotometer, micro-plate reader. To initiate the reaction, 200 μL of the freshly concocted WR reagent (prepared daily by mixing BCA Reagent A and BCA Reagent B in a volume ratio of 50/1) was introduced and left to incubate for a duration of 30 min. The absorbance measurements were recorded at 570 nm. A calibration line, generated using WPC solutions, enabled an estimation of the protein content in the samples. The experiments were repeated on no less than three separate occasions, with the observation that the presence of starch exhibited no interference in the determination of protein levels. The model foulants were used to evaluate the m_o protein, while the residues extracted from the spheres after cleaning were used to evaluate the m_f protein. Tests were made by triplicate.
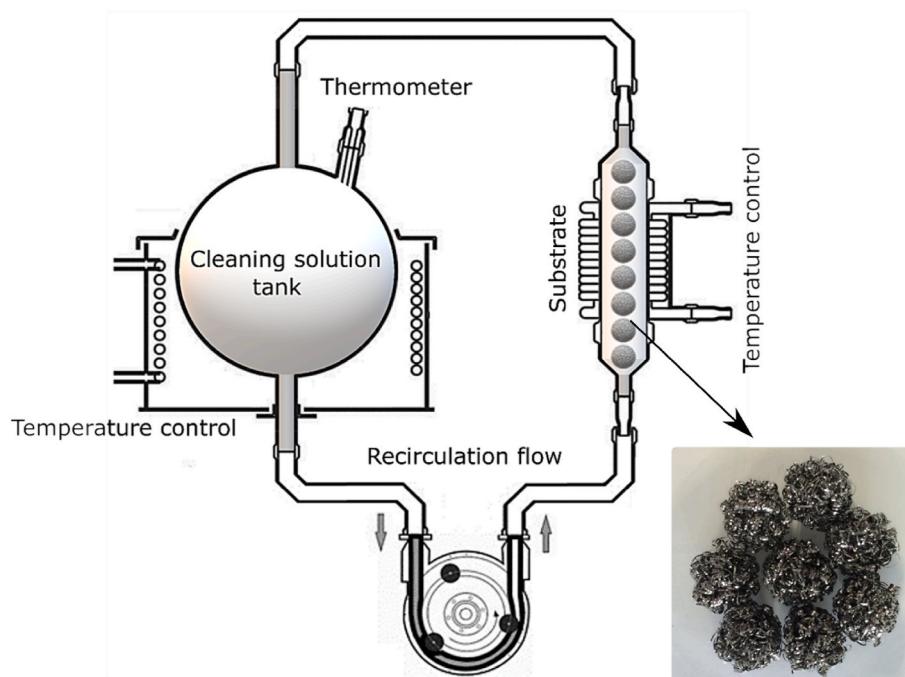

Fig. 2. Lab-simulated Clean-In-Place (CIP) system, comprising a thermostated tank with a volumetric capacity of 1 L, containing the cleaning solution under investigation, a peristaltic pump delivering a continuous flow rate of 120 L/h, and a thermostated glass column (diameter: 2.5 cm, height: 8.5 cm, capacity: 50 mL) where the fouled surfaces were placed. A picture of the substrate is also included. Each cleaning test involved the use of eight spherical coupons.

2.7. Statistical analysis

One-way ANOVA analysis (Gelman, 2005) was conducted to assess statistical differences between datasets. When *p*-value was lower than 0.05, post-hoc Tukey's HSD test was applied to interpret the statistical significance of the difference between two or more means.

3. Mechanical characteristics of model foulants

The mechanical properties and removal mechanisms of the binary mixtures formed by potato starch and whey protein, adhered to stainless steel surfaces, have been systematically studied as a function of temperature (20 and 40 °C) and type of the cleaning solution (pH 7 and pH 13).

Selecting this temperature mid-range enables us to gain better insights into the behaviour of these deposit formulations. The results were analysed along those obtained using a lab-scale Clean-In-Place system to identify any possible correlations that could help to better understand the cleaning process of complex food foulants.

3.1. Viscoelastic properties

Micro-indentation experiments were carried out in ambient (air) at two different temperatures, 20 °C and 40 °C. This preliminary study aimed to analyse the nature of the deposits before embarking on a more comprehensive investigation. Additionally, we sought to establish a potential correlation between cleaning performance and the mechanical properties of the foulant, independent of the cleaning process, in subsequent stages.

Images of the initial and final state of deposits after indentation are shown in Figure SI1. The deposit formed by 100% starch gel (P0) is a translucent semi-rigid gel with compacted macrostructure (Fig. 1 – left image), which is highly affected by temperature. As temperature increased from 20 to 40 °C, deposit dehydration led to the formation of a cracked structure without the influence of any mechanical action (Figure SI1). Once protein was added to the foulant formulation, a visible granular-like structure was identified, being it more pronounced as the ratio of protein increased (Fig. 1). According to literature, high protein concentration favours the formation of larger aggregates (Mleko, 1999; Fickak et al., 2011) due to an increase of the number of cysteine residues that, upon heating, could oxidise and form disulphide bonds that are involved in the cross-linking of proteins (Mleko, 1999). As the testing temperature increased (up to 40 °C), no visual cracking was seen for these protein-containing deposits (i.e., P30–P100).

Fig. 3 shows a schematic representation of a time-resolved indentation evolution (Fig. 3a), along with the indentation force curves recorded (Fig. 3b and **c**). Young's modulus (YM) data are reported in Table 2. Fig. 3 shows that during the approaching phase of the indenter to the air-deposit interface, no force was registered. Once the indenter tip touched the deposit, the indentation force increased. The indentation test concluded once the tip is in contact with the metal surface; force increased rapidly to ca. 5N, shown in Fig. 3a and b.

Among the deposits subjected to testing, P0 exhibited the highest level of hardness (0.21 ± 0.04 MPa; Table 2). Despite the observation of visual cracking in the deposit with an increasing temperature, its Young's modulus (YM) remained largely unaffected by temperature ($p > 0.05$). Notably, a decline in force linearity occurred below a 2 mm displacement, particularly evident with P0, being attributed to the relaxation of the indentation tip (transition from phase II to III; Fig. 3a) and the rupture of the air-foulant interface implying that a hard surface layer had formed. Subsequently, a nearly linear relationship between force and displacement was observed for most of the samples. However, force peaks above 5 mm displacement exhibited partial breakage of the foulant structure during indentation, with these peaks showing greater magnitude at higher temperatures (40 °C). This observation suggests the hypothesis that surface temperature plays a significant role in
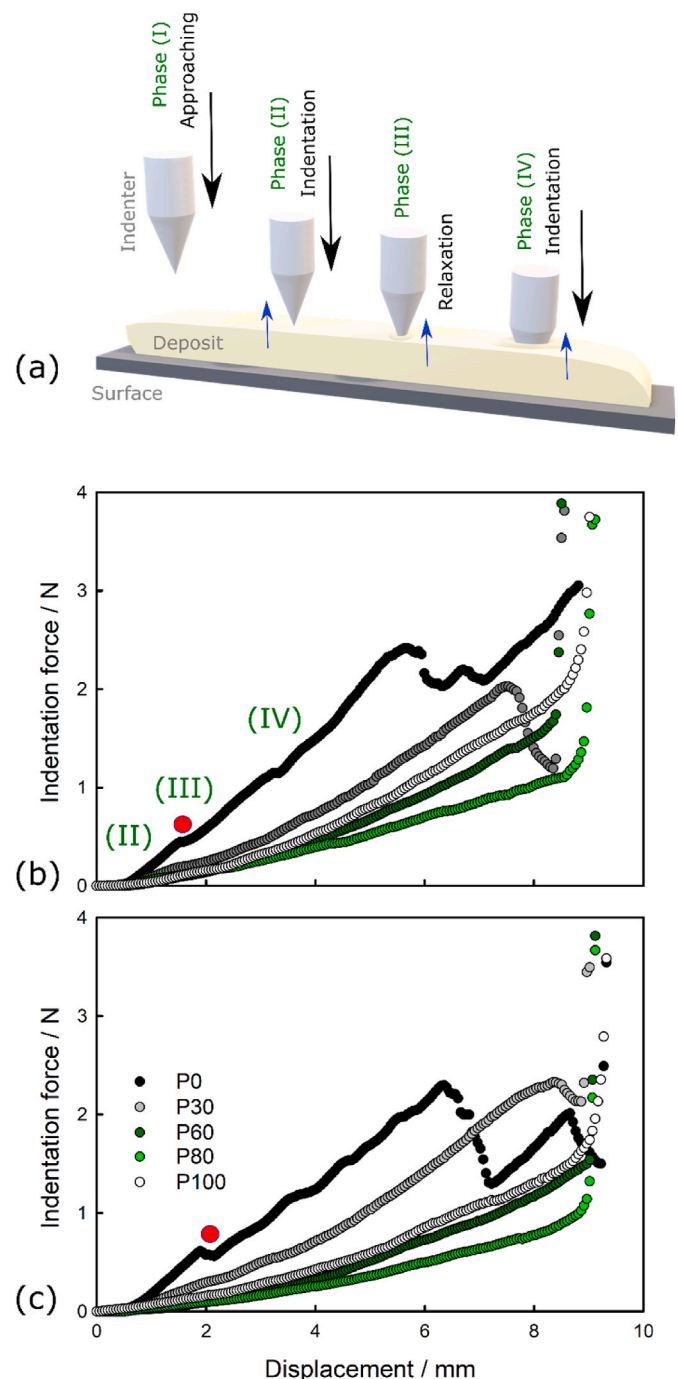
Fig. 3. Micro-indentation experiments: (a) schematic representation of micro-indentation measurements and its phases, and (b and c) representative indentation data (force, N) of the five model foulants *vs.* indenter displacement (mm) at two different temperatures, (b) 20 °C and (c) 40 °C. The red point indicates the breaking of the hard deposit layer formed at the foulant-air interface. A minimum of three measurements were conducted for each condition.

influencing the properties of the deposit's surface in contact with the stainless steel. The heating system used for the samples, which involves convection through the sample holder, initially heating the metal coupon followed by the rest of the foulant. Interestingly, a recent review (Gottschalk et al., 2022), including thermal fouling layers, suggests that thermal history impacts their properties; regions closer to the surface that have experienced prolonged exposure to the surface temperature are particularly susceptible to temperature-induced alterations.

Upon the inclusion of protein in the foulant formulation, a

Table 2
Young modulus data as a function of both the type of foulant and the testing temperature. ANOVA analysis was performed as a function of the deposit temperature, 20 and 40 °C. A minimum of three measurements were conducted for each condition.

Foulant	Young modulus/MPa		ANOVA
	20 °C	40 °C	*p*-value
P0	0.21 ± 0.04	0.20 ± 0.04	0.86
P30	0.13 ± 0.01	0.13 ± 0.02	0.78
P60	0.09 ± 0.01	0.07 ± 0.00	0.35
P80	0.05 ± 0.01	0.04 ± 0.00	0.74
P100	0.11 ± 0.01	0.07 ± 0.01	0.04

discernible trend of softer deposits emerged, evident by a decline in Young's modulus (YM) from 0.21 MPa to 0.13 MPa for P0 and P30, respectively. Notably, while P30 displayed consistent hardness levels at different testing temperatures (20 or 40 °C), analysis of the indentation data revealed that temperature exerted a more pronounced effect as the indenter approached the metal surface, resulting in a reduction in the magnitude of the breakage peak. This suggested a potential enhancement in foulant adhesion with increasing temperature, possibly contributing to the preservation of deposit integrity as a cohesive unit (Figure SI1), contrary to the observed behaviour for P0. Subsequently, as the protein fraction was further augmented (P60-100), YM underwent further reduction, reaching its minimum value for P80 (0.05 MPa). This effect was likely influenced by the starch-protein ratio, as the addition of polysaccharides to whey protein solutions influences the emulsification ability of proteins (Akhtar and Dickinson, 2003, 2007; Zhu et al., 2010), altering the gelatinisation process. Interestingly, the viscoelastic properties of P60 and P80 appeared to be minimally affected by temperature, with both exhibiting similar YM values. In contrast, P100 demonstrated increased stiffness with rising temperature, potentially attributed to two interconnected factors: (i) the absence of starch (with proteins constituting the entire composition), and (ii) the protein concentration, where higher protein content gels tend to be more resistant to penetration compared to those with lower protein concentrations (Fickak et al., 2011).

Although both starch and protein-based deposits belonging to the Type 3 classification (Fryer and Asteriadou, 2009), this section illustrates that their combination and compositional variations yield intriguing and distinct viscoelastic responses when subjected to mechanical stress, which could significantly influence their removal mechanisms, especially during in-place cleaning.

3.2. Micro-mechanical removal

Mechanical removal of the model deposits from stainless steel surfaces through micro-manipulation (section 2.5) involves diverse underlying mechanisms, with the principal failure modes of these deposits graphically depicted in Fig. 4. These failure modes are classified as: (a) adhesive failure, failure at the interface; (b) cohesive failure, occurring within the deposit; (c) dissipative failure, manifesting subsequent to the absorption of energy within the adhesive system; and (d) mixed failure, a combination of distinct failure types. Micro-manipulation measurements were performed under different cleaning conditions (ambient or under chemical treatment) at 20 and 40 °C. Notably, representative images of the deposits after mechanical removal are presented in Figure SI2.

3.2.1. Removal forces of model deposits without chemical action

Fig. 5 shows representative force-time curves, illustrating the adhesion and cohesion characteristics of the rich-in-starch deposits, namely P0 and P30. Both deposits displayed a mixed failure mode, unaffected by either the scraping level or temperature. When the scraper contacted the deposit, elastic deformation ensued at the point of contact, giving rise to an initial dissipative failure (Fig. 4c), followed by complete adhesive failure. For P0, detachment occurred seamlessly as an intact piece, leaving no residues on the metallic substrate. At higher temperature (40 °C), the deposit underwent dehydration, leading to a reduction in the overall removal force, diminishing from 10 mN/mm^2 (~6.5N) to approximately 6 mN/mm^2, thereby facilitating its detachment from the metal surface. This behaviour agrees with the findings reported in section 3.1, where elevated temperatures were found to promote the breakability of P0. Conversely, P30, being softer than P0 (section 3.1),
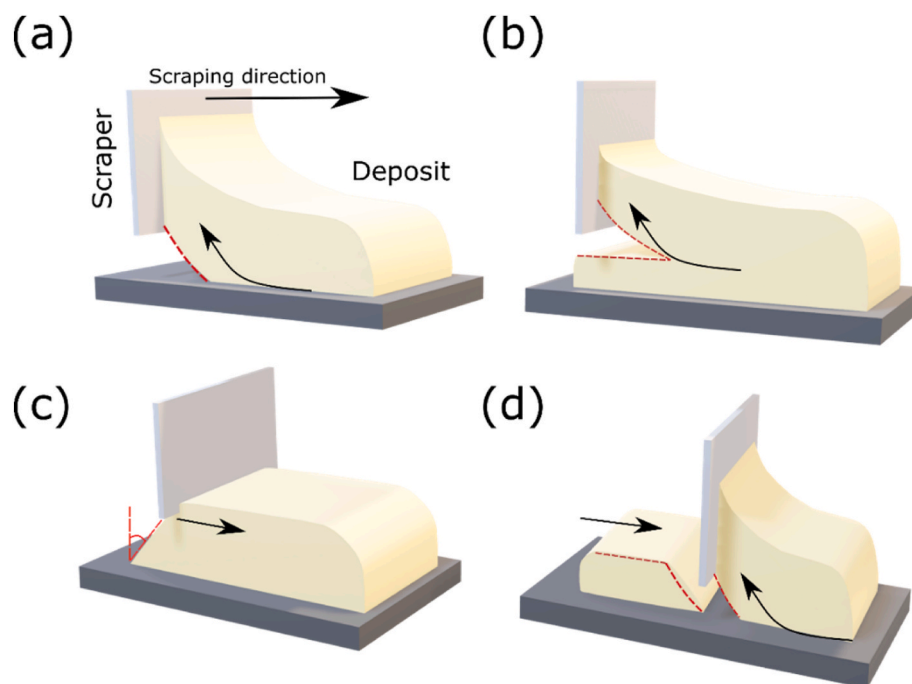
Fig. 4. Schematic representation of the primary types of failures observed during the mechanical elimination of model foulants from stainless steel surfaces, namely: (a) adhesive failure, (b) cohesive failure, (c) dissipative failure, and (d) mixed failure (a distinctive occurrence combining cohesive and adhesive breakages).
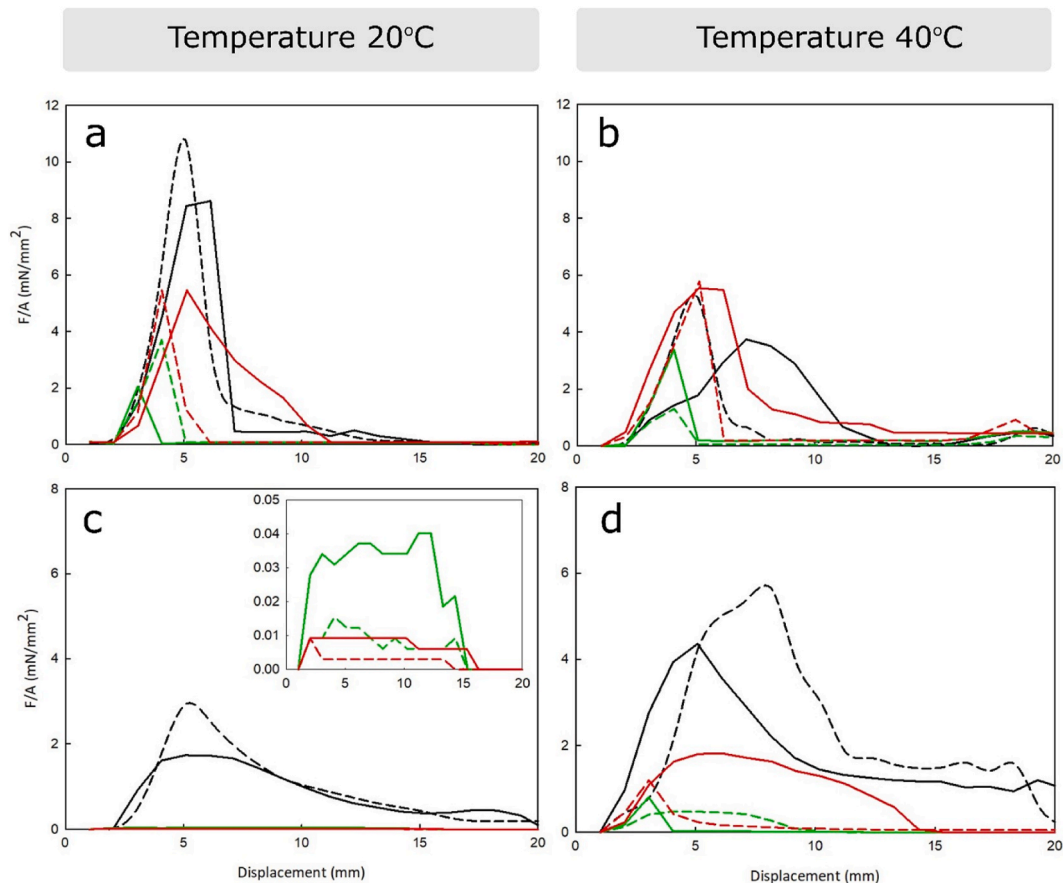
Fig. 5. Representative force-time curves illustrating the "adhesive level" (dashed line) and "cohesive level" (solid line) removal force-displacement curves of model rich-in-starch foulants: (a & b) P0, comprising 100% starch gel at 40 wt%, and (c & d) P30, comprising 70% starch gel at 40 wt% and 30% whey protein gel at 40 wt %. The various testing conditions are represented by distinct line colours: (black) for ambient conditions, (green) for pH 7 buffer, and (red) for pH 13 alkaline solution. The experimental trials were conducted at two dissimilar temperatures: 20 °C (left column) and 40 °C (right column). For enhanced data visualisation, the removal forces for P30 at 20 °C under chemical treatment are displayed in the inner graphs, amplified to a greater scale. At least three repeats were performed per cleaning test.

exhibited a less abrupt adhesive detachment compared to that observed for P0. At the cohesive testing level, the foulant exhibited slight deformation when first contacted by the scraper (dissipative failure), subsequently culminating in a smooth and complete adhesive removal (removal force of ~2.5 mN/mm^2). Even with an increase in temperature, the mechanical response displayed similarities; however, the adhesion forces increased (rising from 2.5 to ~ 6 mN/mm^2), leading to the presence of some adhered pieces of foulant after removal (Figure SI2). This observation aligns with the YM data reported in section 3.1, where proximity to the metal surface and elevated temperatures contributed to a reduced magnitude of the breakage peak, hinting at a possible increase in the foulant's adhesion at higher temperatures, potentially preserving the foulant's structural integrity.

Fig. 6 presents representative force-time curves representing "adhesion" and "cohesion" experiments for rich-in-protein deposits under different temperatures (20 °C and 40 °C). Regardless of the testing temperature, both P60 and P80 exhibit a mixed failure mode, initially experiencing cohesive removal of a foulant layer, followed by a complete adhesive failure, resulting in a complete detachment from the metal surface as a whole. As the protein concentration increases in deposits (P60 and P80), they tend to become softer (section 3.1), leading to a more significant initial indentation by the scraper during testing, specially at higher scraping heights ("cohesion level"), which primarily contributes to the initial cohesive failure. Generally, elevated temperatures appear to promote stronger adhesion of the proteinaceous foulants to the solid substrate (Fig. 6). This, along with a reduction in the Young's

modulus (YM) (section 3.1), can influence deposit removal, leaving more foulant pieces resting on the surface after scraping, especially at "cohesive levels" (Figure SI2). Conversely, the wholly protein deposit (P100) exhibits two distinct removal mechanisms: (i) a mixed failure similar to P60 and P80 (cohesive-adhesive failure) when the scraper is positioned close to the foulant-metal interface, and (ii) cohesive removal when the scraping level is placed 5 mm above the metal surface. As the temperature increases, the YM decreases (by 0.04 MPa) while adhesion increases (by approximately 1 mN/mm^2), resulting in more foulant remnants attached to the surface after removal. Notably, the removal forces for P60 and P100 demonstrate a similar increase as the temperature rises, aligning with the YM reduction reported in section 3.1.

In general, the YM data seem to be consistent with the mechanical removal mechanisms and forces of the model foulants under ambient conditions. While a decrease in YM for rich-in-starch deposits is associated with easier detachment from the metal surface, a reduction in the YM of rich-in-protein deposits requires greater removal forces. Specifically, the removal force for P80 (having the lowest YM) was higher than those needed for P60 and P100. Furthermore, a higher protein content in the binary mixture makes more challenging to achieve complete removal of the deposit (resulting in more material remaining on the surface) after micro-manipulation, despite the removal forces being lower than those required to remove P0.

Fig. 7 presents the maximum shear stress and work per area required to remove the model foulants from stainless steel, with a focus on the cleaning temperature (20 °C and 40 °C). Notably, under ambient
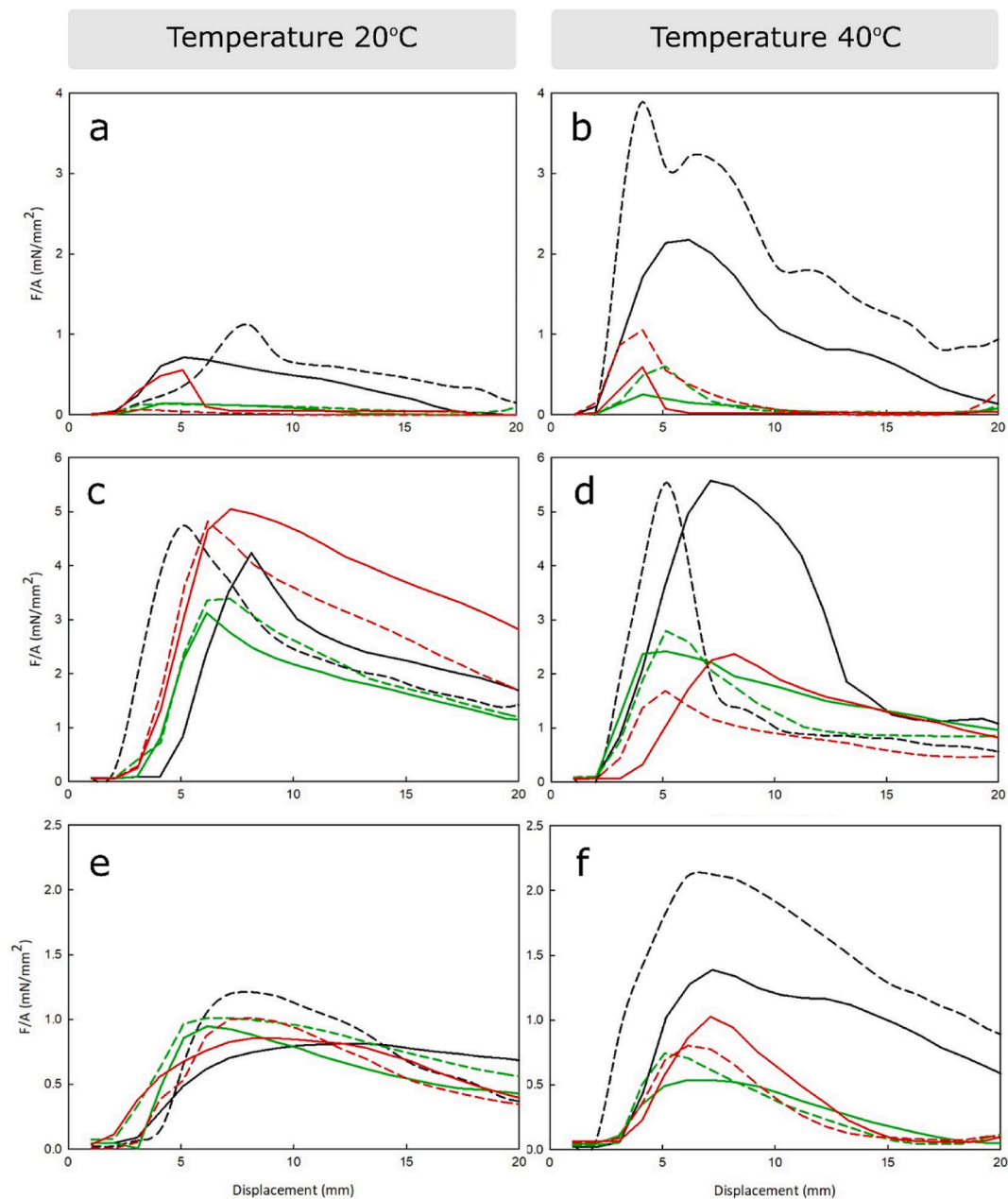
Fig. 6. Representative force-time curves illustrating the "adhesive level" (dashed line) and "cohesive level" (solid line) removal forces of model rich-in-protein foulants: (a & b) P60, consisting of a 40% starch gel at 40 wt% and a 60% whey protein gel at 40 wt%; (c & d) P80, comprising a 20% starch gel at 40 wt% and an 80% whey protein gel at 40 wt%; (e & f) P100, composed of a 100% whey protein gel at 40 wt%. Different testing conditions are represented by line colours: (Black) ambient conditions, (Green) buffer pH 7, (Red) alkaline solution at pH 13. Experiments were conducted at two distinct temperatures: 20 °C (left column) and 40 °C (right column). Each cleaning test was repeated at least three times.

conditions, the maximum shear stress required to remove the model foulants reveals a substantial disparity, with P0 exhibiting higher values compared to the other foulants. Following this, P80 demonstrates a relatively higher stress threshold, while the remaining foulants exhibit comparable stress levels. Upon an increase in temperature, a transformation is observed. The dehydration of P0 induces a drastic reduction in the requisite stress, leading to values akin to those of P30 and P80. However, both P60 and P100 still exhibit lower and quite similar values, suggestive of their distinct behaviour in the context of shear stress. Regarding the removal work data at 20 °C, one deposit (P80) stands out, necessitating more work for its removal compared to all others. Curiously, temperature appears to have limited impact on the removal work at the "cohesive level" (~50 N/m) for P80. However, a slight decrease in

work is observed at the "adhesive level", which can be attributed to the characteristic profile (peak shape) of the force curve (Fig. 6d), bearing resemblance to those displayed by rich-in-starch deposits. Importantly, it should be emphasised that with increasing temperature, the adhesion work for the removal of P30, P60, and P100 increases. This observation may indicate that the elevated temperatures fostered a stronger interfacial adhesion of these samples with the metal substrate, consequently hindering their removal process.

3.2.2. Mechanical removal forces of foulants under chemical treatment

Experiments carried out under pH 7 were served as a control scenario, aiming to investigate the specific influence of the chemical action induced by the alkaline medium at pH 13. At pH 7, both P0 and P30
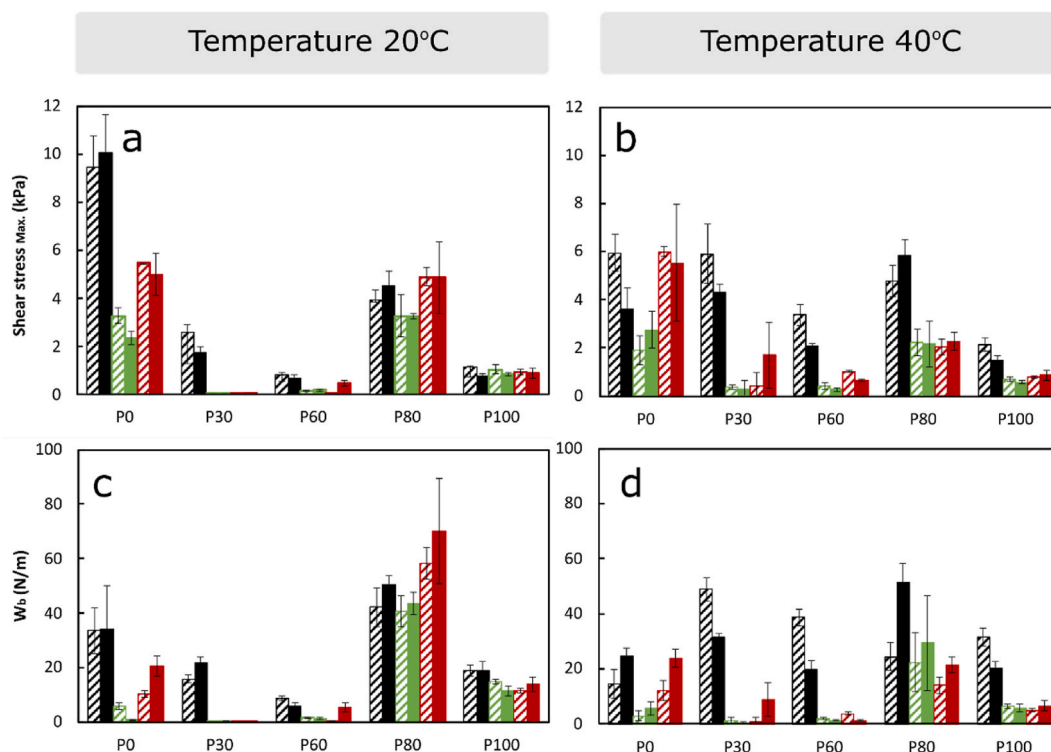
Fig. 7. Maximum shear stress (a & b) and work per area (c & d) to remove model foulants from stainless steel at "adhesive" (dashed bars) and "cohesive" (filled bars) scraping levels as a function of both temperature (20 °C and 40 °C) and cleaning condition: (black line) ambient, (green) phosphate buffer pH 7, and (red) alkaline solution at pH 13. Error bars show the standard deviation of at least three repeats.

exhibit a complete adhesive failure, irrespective of both the scraping level (Fig. 5) and testing temperature, given the absence of foulant dehydration due to immersion in the liquid medium. Notably, for P0, the removal forces remain relatively unchanged across the tested temperature range. Conversely, P30 experiences slight deformation during testing, displaying its removal at very low forces. Upon transitioning to pH 13, the external regions of both foulants demonstrate dissolution (Fig. SI2), yet the overall structure remains intact and adhered to the metal substrate, leading to a complete adhesive failure mechanism, independent of the scraping level, at room temperature. While P0 still experiences a total adhesive failure at the "adhesive level", a mixed failure occurs during "cohesion level" testing, where the deposit breaks at the scraper level, initially in a horizontal manner, but subsequently transitioning diagonally until reaching the metal surface. This behaviour resembles the removal mechanism reported for corn starch-based deposits (Herrera-Marquez et al., 2020). In the case of P30, increasing temperature appears to enhance adhesion, as evidenced by the scraper encountering stepwise indentations due to heightened resistance during removal (Fig. SI2). The increasing swelling of the deposit may also contribute to this effect (Cuckston et al., 2019). At the "cohesion level", the deposit undergoes initial indentation, resulting in deformation and detachment from the metal surface. Nevertheless, some remnants of the foulant persistently remain on the surface even after the removal process.

Independent of temperature, both P60 and P80 show total adhesive failure (low removal forces (Fig. 6), being detached from the metal surface in a whole. At pH 13, greater swelling/dissolution of the external layers of the foulant were observed. However, foulants still detach from the surface in one piece at both scraping levels even though indentation of the scraper into the deposit is more significant at "cohesive" scraping levels. As happened previously, temperature seems to favour swelling, making the scraper go deeper into the deposit. There is still a total adhesive failure at both scraping levels. On the other hand, P80 seems to be softer at higher temperatures despite its removal mechanism not being

significantly affected (adhesive failure). At "cohesive level" (pH 13 and 40 °C), there is a small initial cohesive removal for P80 until a point where there is adhesive failure of the whole deposit (one piece). Finally, at the "cohesion level", P100 shows an initially small cohesive failure followed by a complete adhesive failure independently of temperature. In fact, pH 13 seems to favour swelling of the foulant, it being totally removed by adhesive failure; as happened previously, at "cohesive level", there was an initial cohesive removal followed by a total adhesive failure. Some remaining foulant pieces are still visible in the metal after removal (Figure SI2). When temperature increased, total adhesive failure was observed, with very small indentation at adhesion level. However, as the scraping height was higher, there was some kind of initial cohesive failure, likely favoured by swelling, followed by an adhesive detachment of the foulant from the surface.

In general, the use of chemical treatment reduced the stresses and works required for fouling removal, especially for P0 and P30 at 20 °C, and for most of the foulants at 40 °C (Fig. 7). Based on the findings, it is evident that for P0, the removal work and stresses needed are lower than those observed in an air environment, particularly when a lower pH is used, being it not significantly affected by the cleaning temperature (20 or 40 °C). No significant disparities are apparent in relation to either the cleaning method (pH 7 or pH 13) or temperature for most deposits, with the exception of P80, for which pH 13 seems to slightly decrease the removal work needed at 40 °C.

4. Lab-scale in-place cleaning

As adhesive interactions (section 3.2) between surface and deposit play a dominant role in cleaning efficiency (Otto et al., 2016), a lab-scale Clean-In-Place (CIP) system was used here to better establish the influence of the chemical treatment (neutral and alkaline) on cleaning at 40 °C. This CIP system has a complex substrate formed by stainless steel fibres (section 2.2) that enforces interfacial adhesion.

Detergency results (De) as a function of both the type of cleaning

solution and the foulant composition are shown in Fig. 8 (solid bars). ANOVA analysis (Table 3) was conducted to assess statistical differences between datasets at pH 7 and pH 13. Marked differences were observed as a function of the type of cleaning solution used: cleaning with phosphate pH 7 buffer led to detergency levels lower than 20% for both rich-in-starch foulants (P0 and P30) and for P60, whilst for P80 and P100 detergency reached values ca. 40% and 50% respectively, with cleanliness increasing as the starch content decreases. One of the reasons of this higher removal level could be related to the granular-like structure as the protein fraction increased, where a higher porosity (or cluster dimensions) of the deposit may enhance the transfer of cleaning agents from the bulk solution to the fouling layer and the transfer of reaction products from the fouling layer back to the bulk solution (Ang et al., 2011). At pH 13, detergency of P0, P30 and P60 was significantly enhanced (De > 30%), especially at high starch fractions (De$_{P0}$ = 62.6 ± 8.8%). On the other hand, P80 did not show preferential cleaning with either cleaning solution tested, whilst the removal of the fully protein containing foulant (P100) was drastically increased from 49.9 ± 0.4% (pH 7) to 80.0 ± 6.1% under alkaline treatment.

To determine whether there was preferential cleaning of either protein or starch fractions under the conditions assayed, the protein

Table 3

One-Way ANOVA analysis of Detergency and Protein Cleaning Rate (PCR) of the model deposits as a function of the cleaning solution.

Factor level	Foulant type				
	P0	P30	P60	P80	P100
pH 7 vs. pH 13	$F = 49.3\ p < 0.01$	$F = 51.2\ p < 0.01$	$F = 791.4\ p < 0.001$	$F = 0.6\ p = 0.48$	$F = 72.2\ p < 0.01$

cleaning rate (PCR) was also analysed (Fig. 8; dashed line). This information may be useful to improve cleaning strategies, allowing a preferential removal of specific fraction of the complex deposit. Note that PCR value ranged between 0 and 100% according to the deposit composition. At pH 7, P30 and P80 reached high PCR values, 86.0 ± 10.8 % and 66.9 ± 5.7% respectively, suggesting a protein-dominating removal mechanism where only a small fraction of starch was removed. In contrast, P60 showed a preferential cleaning of starch (PCR 37.2 ± 6.6%). At pH 13, proteinaceous mixtures (P60–P80) showed a cleaning mechanism practically governed by the total removal of proteinaceous material. For P30, it seems to be a preferential removal of starch under alkaline conditions.
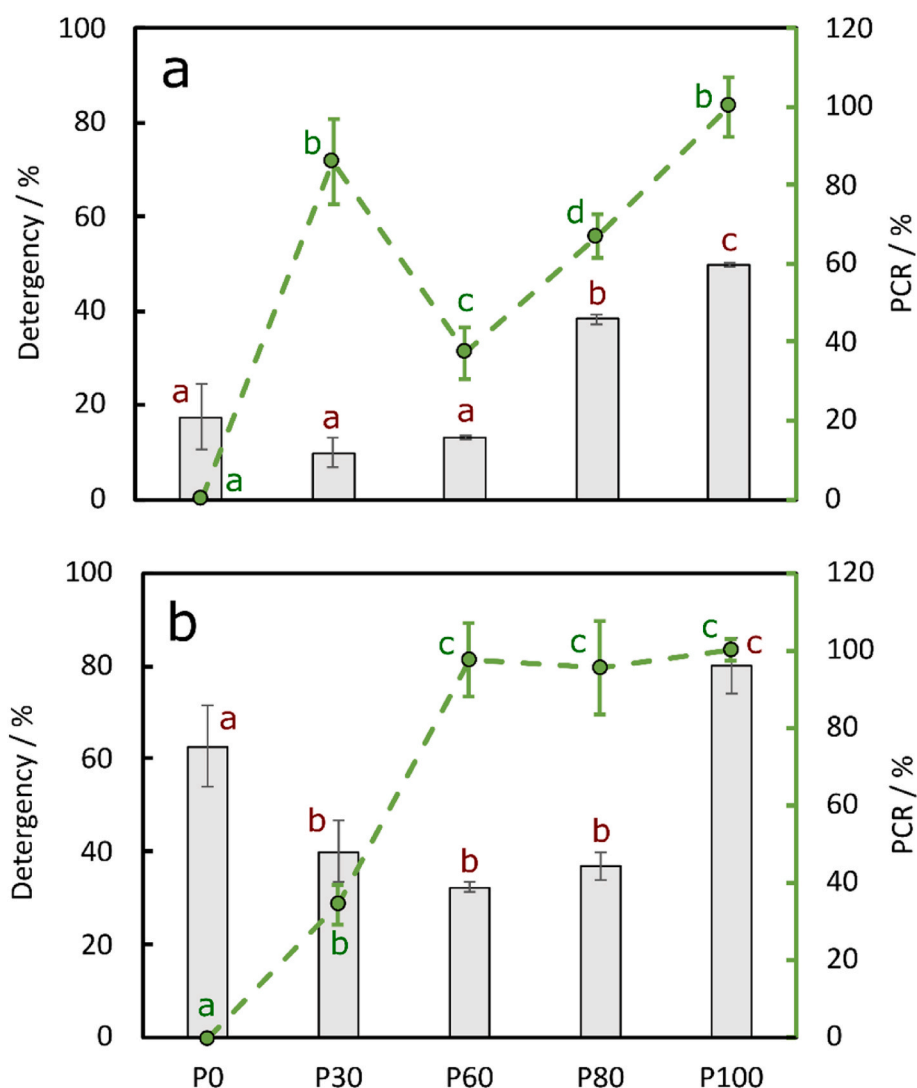
Fig. 8. Detergency (De; solid bars) and Protein Cleaning Rate (PCR; dashed line) of model foulants as a function of the cleaning solution: (a) phosphate buffer pH 7 and (b) alkaline solution at pH 13. Cleaning was performed at a flow rate of 120 L/h for 15 min and 40 °C. Error bars show the standard deviation at least three repeats. When the ANOVA p-value was lower than 0.05, post-hoc Tukey's HSD test was employed to assess the statistical significance of differences between two or more means. Letters denote significant differences (p < 0.05) between datasets for Detergency (red) and PCR (green).

Overall, alkaline cleaning demonstrated a preference for removing most of the model foulants, except for P80, which exhibited similar removal rates under both conditions (pH 7 or pH 13). However, notably, a larger proportion of protein (95.4 ± 12.1%) was removed at high pH. The use of pH 13 was particularly effective in removing protein-based foulants, especially in the case of P100, but it also drastically improved the cleaning of foulants with high starch content, particularly for P0.

Therefore, in-place cleaning shows a distinctive correlation with the mechanical properties of the foulants under study (section 3.1), being highly dependent on both testing temperature and deposit type and composition. This research underscores the complexity of the removal mechanism when dealing with starch-protein mixtures compared to single deposits, highlighting the crucial role that variations in deposit composition during industrial product processing can play in influencing the effectiveness and efficiency of current Clean-in-Place (CIP) protocols.

5. Conclusions

Despite employing starch-based and proteinaceous deposits, both falling under Type 3 classification, their combination and varying compositions resulted in distinctively different viscoelastic responses when subjected to mechanical stress. These responses significantly impact the mechanisms involved in their removal, particularly during in-place cleaning.

In general, the Young's modulus data correlate with the cleaning performance of the model foulants. High-starch content deposits displayed higher levels of hardness, particularly those with lower protein content. Introducing proteins into the foulant formulation revealed a noticeable trend of softer deposits as the protein ratio increased, except in cases where starch was absent, which led to increased deposit hardness. Micro-manipulation results suggest that a decrease in hardness is associated with easier detachment from the metal surface in starch-rich deposits, but it requires greater removal forces for protein-rich deposits, especially in the case of P80. Overall, chemical treatments (pH 7 and pH 13) reduced the mechanical stresses and work required for fouling removal. Alkaline treatment exhibited a preference for removing most of the model foulants, with the exception of P80, which showed similar removal rates under both conditions, pH 7 and pH 13. The intricate cleaning process of P80 appears to be significantly influenced by the interplay between cohesive and adhesive forces, being these forces linked to the deposit type (protein/starch) and composition (protein-starch ratio), along with the potential effects of cleaning parameters (cleaning formulation and temperature) may have on them. Hence, this study highlights the intricacies involved in the removal mechanisms when managing starch-protein mixtures in contrast to single deposits, underscoring the crucial impact that variations in deposit composition during industrial product processing can have on shaping the effectiveness and efficiency of existing Clean-in-Place (CIP) protocols.

CRediT authorship contribution statement

Alejandro Avila-Sierra: Writing – review & editing, Writing – original draft, Visualization, Validation, Supervision, Methodology, Investigation, Formal analysis, Conceptualization. **Raquel Montoya-Guzman:** Validation, Methodology, Formal analysis. **Zhenyu J. Zhang:** Writing – review & editing, Validation, Resources, Project administration, Funding acquisition. **Peter J. Fryer:** Writing – review & editing, Validation, Resources, Project administration, Funding acquisition. **Jose M. Vicaria:** Writing – review & editing, Validation, Supervision, Resources, Project administration, Methodology, Investigation, Funding acquisition, Formal analysis, Conceptualization.

Declaration of competing interest

The authors declare that they have no known competing financial interests or personal relationships that could have appeared to influence the work reported in this paper.

Data availability

Data will be made available on request.

Appendix A. Supplementary data

Supplementary data to this article can be found online at https://doi.org/10.1016/j.jfoodeng.2024.112257.

References

Akhtar, M., Dickinson, E., 2003. Emulsifying properties of whey protein–dextran conjugates at low pH and different salt concentrations. Colloids Surf. B Biointerfaces 31 (1–4), 125–132.

Akhtar, M., Dickinson, E., 2007. Whey protein–maltodextrin conjugates as emulsifying agents: an alternative to gum Arabic. Food Hydrocolloids 21 (4), 607–616.

Ali, A., Alan, Z., Ward, G., Wilson, I., 2015. Using the scanning fluid dynamic gauging device to understand the cleaning of baked lard soiling layers. J. Surfactants Deterg. 18 (6), 933–947.

Ang, W.S., Tiraferri, A., Chen, K.L., Elimelech, M., 2011. Fouling and cleaning of RO membranes fouled by mixtures of organic foulants simulating wastewater effluent. J. Membr. Sci. 376 (1–2), 196–206.

Avila-Sierra, A., Huellemeier, H.A., Zhang, Z.J., Heldman, D.R., Fryer, P.J., 2021a. Molecular understanding of fouling induction and removal: effect of the interface temperature on milk deposits. ACS Appl. Mater. Interfaces 13 (30), 35506–35517.

Avila-Sierra, A., Zhang, Z.J., Fryer, P.J., 2021b. Effect of surface roughness and temperature on stainless steel - whey protein interfacial interactions under pasteurisation conditions. J. Food Eng. 301, 110542.

Bird, M.R., Fryer, P.J., 1991. An experimental study of the cleaning of surfaces fouled by whey proteins. Trans. Inst. Chem. Eng. 69 (Part C), 13–21.

Boxler, C., Augustin, W., Scholl, S., 2013. Cleaning of whey protein and milk salts soiled on DLC coated surfaces at high-temperature. J. Food Eng. 114 (1), 29–38.

Christian, G.K., Fryer, P.J., 2006. The effect of pulsing cleaning chemicals on the cleaning of whey protein deposits. Food Bioprod. Process. 84 (4), 320–328.

Cuckston, G.L., Alam, Z., Goodwin, J., Ward, G., Wilson, D.I., 2019. Quantifying the effect of solution formulation on the removal of soft solid food deposits from stainless steel substrates. J. Food Eng. 243, 22–32.

Eide, M.H., Homleid, J.P., Mattsson, B., 2003. Life cycle assessment (LCA) of cleaning-in-place processes in dairies. LWT–Food Sci. Technol. 36 (3), 303–314.

Fan, L., Chen, X.D., Mercadé-Prieto, R., 2019a. On the nature of the optimum cleaning concentration for dairy fouling: high NaOH concentrations inhibit the cleavage of non-covalent interactions in whey protein aggregates. LWT€"Food Sci. Technol. 101, 519–525.

Fan, L., Ge, A., Chen, X.D., Mercadé-Prieto, R., 2019b. The role of non-covalent interactions in the alkaline dissolution of heat set whey protein hydrogels made at gelation pH 2–11. Food Hydrocolloids 89, 100–110.

Fickak, A., Al-Raisi, A., Chen, X.D., 2011. Effect of whey protein concentration in the fouling and cleaning of a heat transfer surface. J. Food Eng. 104, 323–331.

Fryer, P.J., Asteriadou, K., 2009. A prototype cleaning map: a classification of industrial cleaning processes. Trends Food Sci. Technol. 20, 255–262.

Fryer, P.J., Robbins, P.T., Cole, P.M., Goode, K.R., Zhang, Z., Asteriadou, K., 2011. Populating the cleaning map: can data for cleaning be relevant across different lengthscales? Procedia in Food Science 1, 1761–1767.

Gelman, A., 2005. Analysis of variance—why it is more important than ever. Ann. Stat. 33, 1–53.

Gottschalk, N., Augustin, W., Scholl, S., Wilson, I., Mercadé-Prieto, R., 2022. Model food soils for investigating cleaning: a review. Food Bioprod. Process. 136, 249–296.

Han, J.A., Lim, S.T., 2004. Structural changes in corn starches during alkaline dissolution by vortexing. Carbohydr. Polym. 55 (2), 193–199.

Heldman, D.R., 2021. Sustainability of the food supply chain; energy, water and waste. Food Engineering Innovations across the Food Supply Chain, pp. 47–60.

Herrera-Marquez, O., Serrano-Haro, M., Vicaria, J.M., Jurado, E., Fraatz-Leál, A.R., Zhang, Z.J., Fryer, P.J., Avila-Sierra, A., 2020. Cleaning maps: a multi length-scale

strategy to approach the cleaning of complex food deposits. J. Clean. Prod. 261, 121254.

Huellemeier, H.A., Eren, N.M., Payne, T.D., Schultz, Z.D., Heldman, D.R., 2022. Monitoring and characterization of milk fouling on stainless steel using a high-pressure high-temperature quartz crystal microbalance with dissipation. Langmuir 38 (31), 9466–9480.

Jennings, W.G., 1965. Theory and practice of hard-surface cleaning. Bd. 14. In: Chichester, C.O., Stewart, G.F., Mrak, E.M. (Eds.), Advances in Food Research, vol. 14. Academic Press, pp. 325–458. Bd. 14.

Jurado-Alameda, E., Herrera-Marquez, O., Martínez-Gallegos, J.F., Vicaria, J.M., 2015. Starch-soiled stainless steel cleaning using surfactants and a-amylase. J. Food Eng. 160, 56–64.

Jurado, E., Herrera-Marquez, O., Plaza-Quevedo, A., Vicaria, J.M., 2015. Interaction between non-ionic surfactants and silica micro/nanoparticles. Influence on the cleaning of dried starch on steel surfaces. J. Ind. Eng. Chem. 21, 1383–1388.

Lai, L.N., Karim, A.A., Norziah, M.H., Seow, C.C., 2004. Effects of Na2CO3 and NaOH on pasting properties of selected native cereal starches. J. Food Sci. 69, 249–256.

Landel, J.R., Wilson, D.I., 2021. The fluid mechanics of cleaning and decontamination of surfaces. Annu. Rev. Fluid Mech. 53, 147–171.

Langley, K.R., Green, M.L., 1989. Compression and impact strength of gels, prepared from fractionated whey proteins, in relation to composition and microstructure. J. Dairy Res. 56, 275–284.

Liu, W., Christian, G.K., Zhang, Z., Fryer, P.J., 2002. Development and use of a micromanipulation technique for measuring the force required to disrupt and remove fouling deposits. Food Bioprod. Process. 80, 286–291.

Magens, O.M., Liu, Y., Hofmans, J.F.A., Nelissen, J.A., Wilson, D.I., 2017. Adhesion and cleaning of foods with complex structure: effect of oil content and fluoropolymer coating characteristics on the detachment of cake from baking surfaces. J. Food Eng. 197, 48–59.

Mercadé-Prieto, R., Wilson, D.I., Paterson, W.R., 2008. Effect of the NaOH concentration and temperature on the dissolution mechanisms of ß-lactoglobulin gels in alkali. Int. J. Food Eng. 4 (5), 9.

Mleko, S., 1999. Effect of protein concentration on whey protein gels obtained by a two-stage heating process. Eur. Food Res. Technol. Z Lebensm. Unters. Forsch. 209, 389–392.

Nor Nadiha, M.Z., Fazilah, A., Bhat, R., Karim, A.A., 2010. Comparative susceptibilities of sago, potato and corn starches to alkali treatment. Food Chem. 121, 1053–1059.

Otto, C., Zahn, S., Hauschild, M., Babick, F., Rohm, H., 2016. Comparative cleaning tests with modified protein and starch residues. J. Food Eng. 178, 145–150.

Palanisamy, A., Moulin, G., Ramaioli, M., Plana-Fattori, A., Flick, D., Menut, P., 2022. Determination of the mechanical properties of gelatinized starch granule from bulk suspension characterization. Rheol. Acta 61, 299–308.

Saenz-Espinar, M.J., Arroyo-Camarena, M., Vicaria, J.M., Luzón, G., Ávila-Sierra, A., 2024. Multi-length scale approach to investigate cleaning of food-derived deposits adhered to hard surfaces: mixtures of starch, whey protein, and lard. Food Bioprocess Technol. https://doi.org/10.1007/s11947-024-03330-2.

Schug, D., 2016. Reducing water usage in food and beverage processing. Food Engineering. April. In: www.foodengineeringmag.com/articles/95493-reducing-water-usage-in-food-and-beverage-processing.

Sneddon, I.N., 1948. Boussinesq's problem for a rigid cone. Math. Proc. Camb. Phil. Soc. 492–507.

Tanaka, A., Hoshino, E., 1999. Study on the substrate specificity of α-amylases that contribute to soil removal in detergents. J. Surfactants Deterg. 2 (2), 193–199.

Tuladhar, T.R., Paterson, W.R., Wilson, D.I., 2002. Investigation of alkaline cleaning-in-place of whey protein deposits using dynamic gauging. Food Bioprod. Process. 80 (3), 199–214.

Van Asselt, A.J., Vissers, M.M.M., Smit, F., De Jong, P., 2005. In-line control of fouling, heat exchanger fouling and cleaning—challenges and opportunities. In: Engineering Conferences International Kloster Irsee, Germany, 5-10 June (Engineering Conferences International, New York, USA).

Vicaria, J.M., Jurado-Alameda, E., Herrera-Marquez, O., Olivares-Arias, V., Avila-Sierra, A., 2017. Analysis of different protocols for the cleaning of corn starch adhering to stainless steel. J. Clean. Prod. 168, 87–96.

Von Rybinski, W., 2007. Physical aspects of cleaning processes. In: Johannson, I., Somasundaran, P. (Eds.), Handbook for Cleaning/Decontamination of Surfaces. Elsevier, pp. 1–I.

Wilson, D.I., Christie, G., Fryer, P.J., Hall, I.M., Landel, J.R., Whitehead, K.A., 2022. Lessons to learn from roadmapping in cleaning and decontamination. Food Bioprod. Process. 135, 156–164.

Zhu, L.J., Shukri, R., de Mesa-Stonestreet, N.J., Alavi, S., Dogan, H., Shi, Y.C., 2010. Mechanical and microstructural properties of soy protein – high amylose corn starch extrudates in relation to physiochemical changes of starch during extrusion. J. Food Eng. 100 (2), 232–238.